

# LASER DOPPLER ANEMOMETRY STUDY OF THE FLOW IN A BLOOD FILTER

## Rudolf Huebner

Universidade Federal de Minas Gerais – Departamento de Engenharia Mecânica  
Av. Antônio Carlos, 6627 – Pampulha – BH – MG - CEP 31270-901  
[rudolf@demec.ufmg.br](mailto:rudolf@demec.ufmg.br)

## Paolo Castellini

Università degli Studi di Ancona  
Via Breccie Bianche, 60131 – Ancona – Italia  
[cast@mehp1.unian.it](mailto:cast@mehp1.unian.it)

## Marcos Pinotti Barbosa

Universidade Federal de Minas Gerais – Departamento de Engenharia Mecânica  
Av. Antônio Carlos, 6627 – Pampulha – BH – MG - CEP 31270-901  
[pinotti@demec.ufmg.br](mailto:pinotti@demec.ufmg.br)

## Ricardo Schayer Sabino

Universidade Federal de Minas Gerais – Departamento de Engenharia Mecânica  
Av. Antônio Carlos, 6627 – Pampulha – BH – MG - CEP 31270-901  
[schayer@demec.ufmg.br](mailto:schayer@demec.ufmg.br)

**Abstract.** *Damage to red blood cells can be induced chemically, by osmosis or mechanically. The fluid mechanical effect can be related to the device design, its surface characteristics and to the degree of flow disturbance or turbulence caused by the device. It is generally accepted that the presence of high turbulent shear stresses generated in the flow fields of artificial devices are partially responsible for the levels of red blood cells destruction, or hemolysis. Investigating the effect of turbulent shear stress on hemolysis is of prime importance to research work related to artificial devices. Hemolysis is a function of the shear stresses magnitude acting on blood cells and their exposure time to the shear stresses. The present work presents the use of two techniques used to study the flow in an arterial blood filter. The general structure of the flow field was analyzed using the dye injection technique. A laser Doppler anemometer was used to measure two orthogonal velocity components and their fluctuations, which were used to determine the turbulent shear stresses. The exposure time was calculated and used in conjunction with the turbulent shear stresses to estimate the hemoglobin released by the red blood cells.*

**Keywords.** *Blood filter, LDA, Visualization, Hemolysis, Turbulence*

## 1. Introduction

Nowadays cardiopulmonary bypass (CPB) with extracorporeal blood oxygenation is a very common practice. Microembolization occurs during CPB due to the presence of bubbles air, thrombi, platelet aggregates and pieces of plastic into the arterial line as cited by Waaben *et al.* (1994). Microemboli can cause organ dysfunction, especially in the brain, liver, lung and kidney. The use of a blood filter in the arterial line of the extracorporeal circuit has been one of the proposed methods to retain microemboli thus avoiding organ dysfunction.

Blood flow through artificial devices (heart valves, blood pumps, oxygenators and filters) is associated with thrombus formation and hemolysis (red blood cell damage). Hemolysis is one of the most difficult problems encountered in extracorporeal circulation. The mechanism that causes red blood cell damage is not completely clear, namely the relationship between hemolysis and blood flow behavior. Flow behavior is considered in terms of pressure levels, turbulence intensity, flow acceleration and stagnation. Elevated Reynolds stresses produced by turbulent flows have been associated with red blood cell damage.

Damage to blood corpuscles can be induced chemically, by osmosis or mechanically. The fluid mechanical effect can be related to the device design, surface characteristics and degree of flow disturbance. Flow properties, most notably turbulence, shear stress and stagnation, have been implicated in several artificial devices problems including blood cell damage, thrombus formation, calcification and infection. Damage of blood cells associated with elevated shear stresses and prolonged exposure of cells are the underlying fluid mechanical mechanisms which must be understood in order to improve the artificial devices design.

Red blood cells damage can be induced at moderate shear stress in the presence of a foreign surface, as shown by Sutura and Mehrjardi (1975). Sutura (1977) has shown that prolonged exposure to turbulent shear stresses as low as 150 N/m<sup>2</sup> can produce lysis of red blood cells. Sallam and Hwang (1984) have shown that incipient hemolysis begins at Reynolds stresses of about 400 N/m<sup>2</sup>. The resistance of red blood cells to shearing forces is higher than was assumed, reaching a threshold of 500 N/m<sup>2</sup> for 1 s of exposure (Paul *et al.*, 1999).

Constant stress experiments have demonstrated that the critical level of shear stress tolerable by a cell is highly depend upon the time of exposure. Rand (1964) describes one possibility to correlate shear stress and exposure time is to describe blood trauma by the mathematical relation  $\tau^2.t = \text{constant}$  where  $\tau$  is the shear stress and  $t$  the exposure time. This equation is comparable to the equation proposed by Wurzing *et. al* (1985) which is an empirical correlation

based on experimental data using a Couette viscometer. In this equation the percentage of released hemoglobin is given by

$$\frac{\Delta\text{Hb}}{\text{Hb}} \% = 3.62 \times 10^{-5} t^{0.785} \tau_{\text{max}}^{2.416} \quad (1)$$

where  $t$  is the residence time (in s) and  $\tau_{\text{max}}$  is the maximum turbulent shear stress (in  $\text{N/m}^2$ ). In this work the equation above was used to evaluate the free hemoglobin percentage in an arterial blood filter. The aim of this work is to study the flow structure in an arterial blood filter. Some regions of the filter were studied using the laser Doppler velocimetry technique and velocity profiles and their fluctuations are presented. Turbulent stresses and blood cells exposure time were evaluated and used to estimate the hemolytic potential associated to the flow structure.

## 2. Materials and Methods

### 2.1. The blood filter

The filter studied in used in cardiopulmonary bypass procedures. The body filter is made using acrylic and a polyester screen is used in the filtering element. The filtering element has a porosity of  $40 \mu\text{m}$ . The filter inlet and outlet connectors have a diameter of  $9,5 \text{ mm}$  and are made of reinforced acrylic. The filter has a priming volume of about  $280 \text{ ml}$ , is project to be used in adult patients and can be operated with a maximum flow rate of  $6 \text{ liters per minute}$ . The filter has a bypass line that can be used in situations where the filtering element pores are closed and another line is used to eliminate air trapped by the filter. Figure 1 shows a schematic view of the filter, its elements and how it works. In figure 1, blue arrows are used to indicate unfiltered blood while red arrows indicate filtered blood

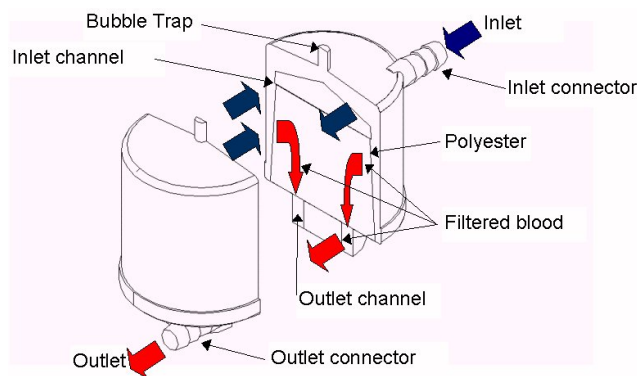


Figure 1. Schematic view of the filter

Blood flows through the inlet connector, located at the upper part of the filter, and describes a descending helical movement while it flows along the inlet channel. During this helical movement the blood flows through the filtering element, polyester, reaches the outlet channel and flows in direction of the outlet connector, located at the bottom of the filter.

### 2.2. The flow circuit

A test bench was assembled in order to reproduce the flow condition observed during a cardiopulmonary bypass. Figure 2 depicts schematically the test circuit.

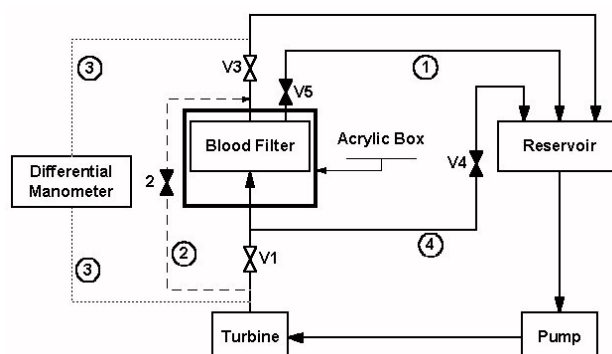


Figure 2 – Schematic view of the test circuit

Working fluid was pumped through the turbine and blood filter returning to the circuit reservoir. Line 1 represents the bubble trap and was used during the circuit filling up. During the LDA measurements many particles, necessary due to the LDA working principle, were captured by the filtering element and Lines 2 and 4 were used together to clean the filter using a retrograde flow. Pressure drop across the filter was monitored by a differential manometer, indicated by the lines 3. Flow rate was monitored by a turbine flow meter and the pump rotating speed was controlled changing the excitation voltage of a brushless motor. All elements were connected using PVC flexible tubes. A prismatic acrylic box was used as optical window to minimize optical distortions. During the LDA measurements and flow visualization tests the filter was placed inside this prismatic box filled with water. The flow rate used in the LDA tests was 4.5 liters per minute which is in accordance with the values used during a cardiopulmonary bypass. The flow was seeded with  $Al_2O_3$  particles with a mean measured diameter of  $48 \mu m$ . Water was used during the visualization tests using dye injection and the flow rate was estimated using Reynolds similitude between water and the water-glycerin solution.

### 2.3. Laser Doppler anemometry

A two-component fiber optic laser Doppler anemometer (DANTEC) was used to measure the axial and tangential velocity components. In this system a 4 W argon-ion laser was coupled to a fiber drive unit which allowed for a color separation of the primary beam. The resulting green (514.5 nm wavelength) and blue (488 nm wavelength) beams were used for the velocity measurements. A 160 mm focal length lens was coupled to the LDA probe to produce an ellipsoidal measurement volume with a maximum length, in air, of 0.658 mm and a diameter of 0,078 mm. The Doppler signal were processed with fast Fourier signal analyzer and a commercial software (Burstware) was used to acquire data and to control the signal analyzers and the photomultiplier. Approximately 3000 measurements were acquired for each spatial location. LDA measurements were done at four different planes labeled N, S, E and O and each plane was divided in eight levels. A coordinate system was adopted in order to perform the measurements. The system is oriented in such a way that x axis is directed radially, y axis axially and z axis is tangential to the filter. Z axis is horizontally directed and always parallel to the LDA probe surface. Figure 3 shows the measurement planes and the coordinate system used during the LDA measurements. The first level was located 13 mm above the intersection of the bottom piece with the lateral piece of the filter and the next level was placed 5 mm above the previous. The tangential velocity (U) is positive in the negative sense of the z axis while the axial velocity (V) is positive following the y axis sense.

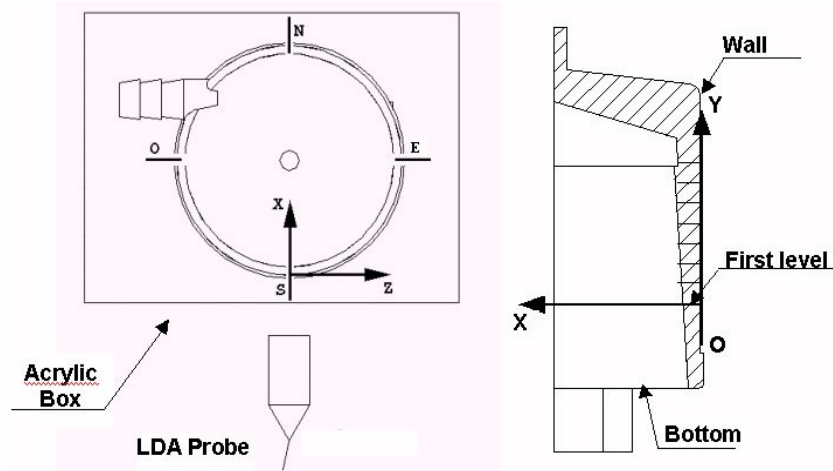


Figure 3 – Coordinate systems and measurements planes

The working fluid was a combination of 40%, in mass, of glycerin with 60% of water. This working fluid was chosen because it matches the blood transport properties. At  $25^{\circ}C$ , the blood analog fluid has a density of  $1.09 \text{ g/cm}^3$  and absolute viscosity of  $3.18 \text{ mPa}\cdot\text{s}$ . One problem associated with this working fluid when using an optical measurement technique is the refraction index. The measured refraction index of the solution was 1.383 which is lower than 1.49, the refractive index of the filter wall. This difference implies in a displacement of the LDA measurement volume due to the refraction of the laser beams. An equation that describes the position of the measurement volume inside the filter was developed using Snell's law. Figure 4 shows the refraction of two laser beams crossing to materials with different refraction index. The beams should be intercepted at O but they are intercepted at O' due to the difference between  $n_1$  and  $n_2$ , the materials refraction indexes.

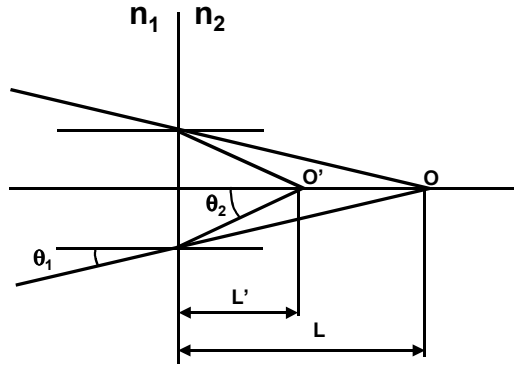


Figure 4 – Laser beams crossing two different materials

The equation that describes the correct position of the measurement volume is where  $\theta_2$  is evaluated using Snell's law (Dybbs and Edwards, 1987).

$$\frac{L'}{L} = \frac{\tan \theta_1}{\tan \theta_2} \quad (2)$$

The instantaneous velocities ( $\tilde{u}_n$  and  $\tilde{v}_n$ ), measured by the LDA, can be separated into mean components (U and V) and fluctuating components ( $u_n$  e  $v_n$ ). Mean velocities can be evaluated as

$$\bar{U} = \frac{I}{N} \sum_I^N \tilde{u}_n \quad (3)$$

and

$$\bar{V} = \frac{I}{N} \sum_I^N \tilde{v}_n, \quad (4)$$

where N is the number of collected samples. The fluctuating components are estimated using equations (5) and (6).

$$u_n = \tilde{u}_n - \bar{U} \quad (5)$$

and

$$v_n = \tilde{v}_n - \bar{V}. \quad (6)$$

The gate-time averaging technique was adopted in order to remove the “velocity bias” which, would lead to the overestimation of the velocity. Techniques for determining Reynolds stresses in stationary flows from LDA measurements are well established (Baldwin et al, 1993). Reynolds normal stresses ( $\overline{\rho u u}$  e  $\overline{\rho v v}$ ) and shear stress ( $\overline{\rho u v}$ ) are determined by the following equations.

$$\overline{\rho u u} = \frac{I}{N} \sum_I^N \rho u_n^2, \quad (7)$$

$$\overline{\rho v v} = \frac{I}{N} \sum_I^N \rho v_n^2, \quad (8)$$

and

$$\overline{\rho u v} = \frac{I}{N} \sum_I^N \rho u_n v_n. \quad (9)$$

Normal and shear stresses were used to evaluate principal stresses. Principal stresses are estimated using the equation proposed by Higdon et al (1985)

$$\bar{\sigma}_{max,min} = \frac{\overline{\rho uu} + \overline{\rho vv}}{2} \pm \sqrt{\left(\frac{\overline{\rho uu} - \overline{\rho vv}}{2}\right)^2 + \overline{\rho uv}^2}, \quad (10)$$

and the maximum shear stress can then be obtained from the principal stresses as

$$\tau_{max} = \frac{1}{2}(\sigma_{max} - \sigma_{min}) \quad (11)$$

The magnitude of shear stresses acting on red blood cells and their exposure times to that shear fields are two parameters that have to be considered in the study of hemolysis induced by the flow. In the present work the exposure time was estimated considering the time necessary to the seeding particles to cross the LDA measurement volume. The percentage of hemoglobin released by red blood cells was evaluated using the equation proposed by Wurzinger et al (1985)

$$\%Hb = 3,62 \times 10^{-5} t^{0.79} \tau_{max}^{2.4} \quad (12)$$

where  $t$  is the exposure time, in seconds, and  $\tau_{max}$  is the maximum shear stress, in  $N/m^2$ . The turbulent kinetic energy was evaluated using the following equation.

$$ECT = \frac{u^2 + v^2}{2} \quad (13)$$

## 2.4. Flow visualization

Flow visualization was done using the same test bench described before. Dye was injected, using a needle, through the inlet connector and eight orifices made at the upper part of the filter. At each orifice the dye was injected at three different levels. Figure 5 shows the injection points and levels. It must be pointed out that the nomenclature used to label the measurement planes was adopted to the injection points. Visualization was performed using a WEB camera placed normal to the filter wall in the region where the needle was placed.



Figure 5 – Injection points and levels

Water, at 25°C, was used as working fluid and Reynolds similitude was used to evaluate the flow rate. The characteristic length used in the Reynolds number evaluation was the diameter of the inlet connector.

$$Re_{water} = Re_{sol.40\%} \quad (13)$$

and so

$$\frac{\rho_{water} V_{water} D_{filter}}{\mu_{water}} = \frac{\rho_{sol.40\%} V_{sol.40\%} D_{filter}}{\mu_{sol.40\%}} \quad (14)$$

Water flow rate can be expressed in terms of water-glycerin flow rate and kinematics viscosity as

$$Q_{water} = \frac{v_{water}}{v_{sol.40\%}} Q_{sol.40\%} = \frac{0,857}{2,898} 4,5 = 1,33 \quad (15)$$

The flow rate used was 1,33 l/min. The similitude asserts that the flow pattern observed using water is the same that using the solution of water and glycerin.

### 3. Results and Discussion

#### 3.1. Flow visualization

Figure 6 shows the flow visualization, at the upper part of the filter, at different instants of time. The left image shows a dye jet flowing through the inlet connector and achieving the opposite wall. The jet is deflected and tends to flow in direction of the E plane. At the left image is possible to see that the jets flows in a clockwise sense and finally achieves the inlet connector. There is a white spot near the central region of the filter. This spot shows a recirculating flow which difficults the convective mass transport and the dye dispersion.



Figure 6 – Flow visualization at the upper part of the filter at two different instants of time

Flow visualization at planes E, SE, S and SO is show at figure 7, respectively. At planes E and SE dye flows in a descending clockwise sense, showing that the velocity vector has at least two components, the tangential and axial. At planes S and SO the axial component vanishes and the dye flows horizontally. Figure 8 shows the flow visualization at planes O, NO, N and NE, respectively. At planes O and NO the flow has an ascending behavior, this mean that the axial velocity has a positive value and the blood is not collected by the outlet channel. Dye flows vertically at plane N and this phenomenon will be explained combining the information from planes NO and NE. The visualization at plane NE shows the incoming jet being divided because part of the dye flows in a clockwise sense, in direction of plane E while part of it flows in direction of the N plane. The flow coming from the NE plane will interact with the flow coming from the NO plane and this fact combined with low pressure area created by the presence of the incoming jet, near the plane NO where the inlet connector is present, explains the flow behavior at plane N.



Figure 7 – Flow visualization at planes E, SE, S and SO, respectively

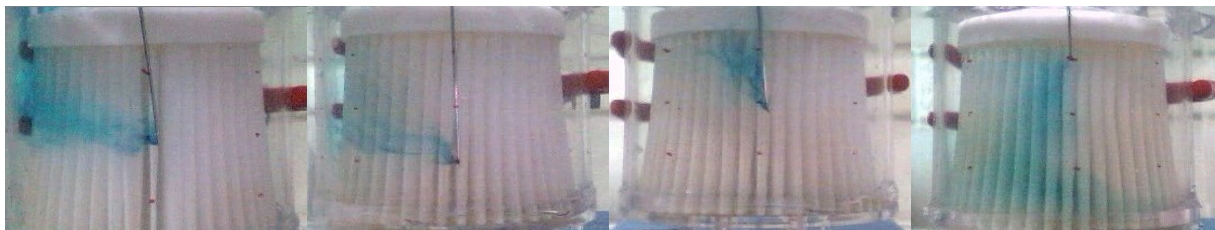


Figure 8 – Flow visualization at planes O, NO, N and NE, respectively

### 3.2. LDA measurements

Figure 9 shows the tangential velocity isocurves at the four planes. The velocity has a maximum value, absolute value, of 0,64 m/s at plane E which decreases until 0,17 m/s at plane N. In all planes the velocity decreases radially, it presents a maximum value near the wall which decreases near the filtering element.

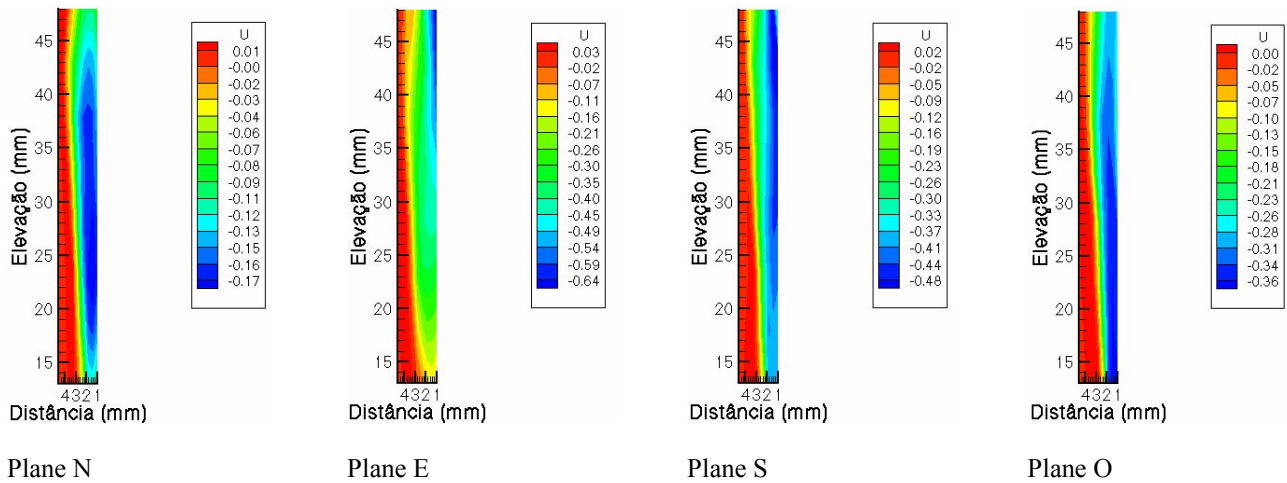


Figure 9 – Tangential velocities (m/s) at the four planes

At the plane O the velocity increases with the elevation decreasing. In all planes is possible to see a reversal flow at region near the filtering element, because the velocity is negative near the wall and positive near the polyester. In figure 10 is possible to see the axial velocity at the four planes. At the plane N the component is positive and indicates an ascending flow as shown by the third picture in figure 8. The flow has a descend behavior in plane E because the velocity is negative. In planes S and O the flow is descend near the wall and ascending near the filtering element indicating a reversal flow in this planes.

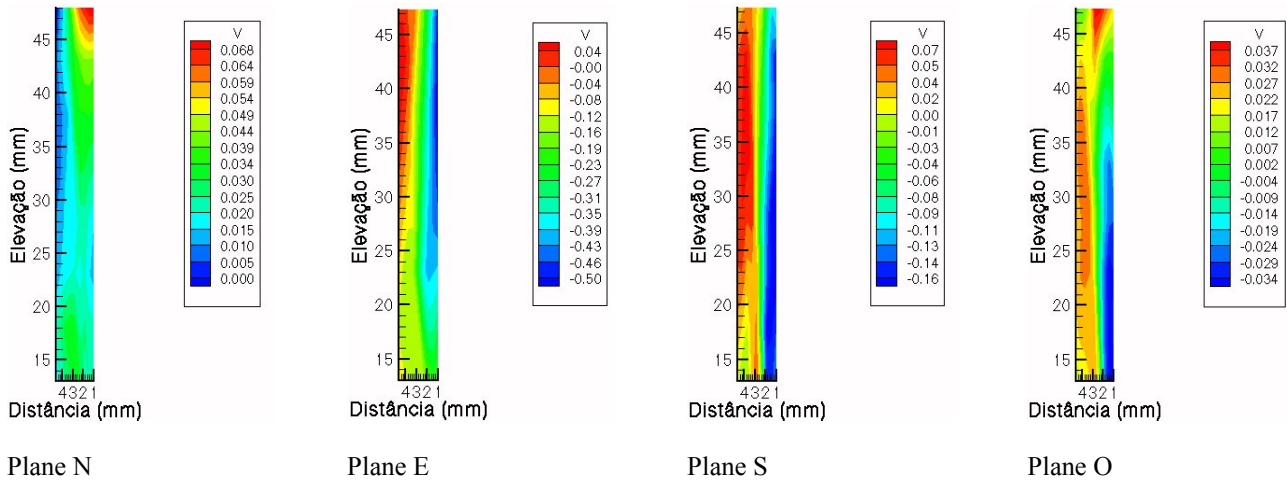


Figure 10 – Axial velocities (m/s) at the four planes

Figure 11 shows the turbulent kinetic energy in the four planes. It has a maximum value in plane E due to the proximity of the point where the incoming jet changes flow direction. The presence of the jet can be observed at plane S because in this plane the turbulent kinetic energy has a maximum value of  $1.29E-02 \text{ m}^2/\text{s}^2$  at 48 mm. In planes N and O the turbulent kinetic energy decreases showing that mostly of the jet energy is transferred to the flow at the planes E and S.

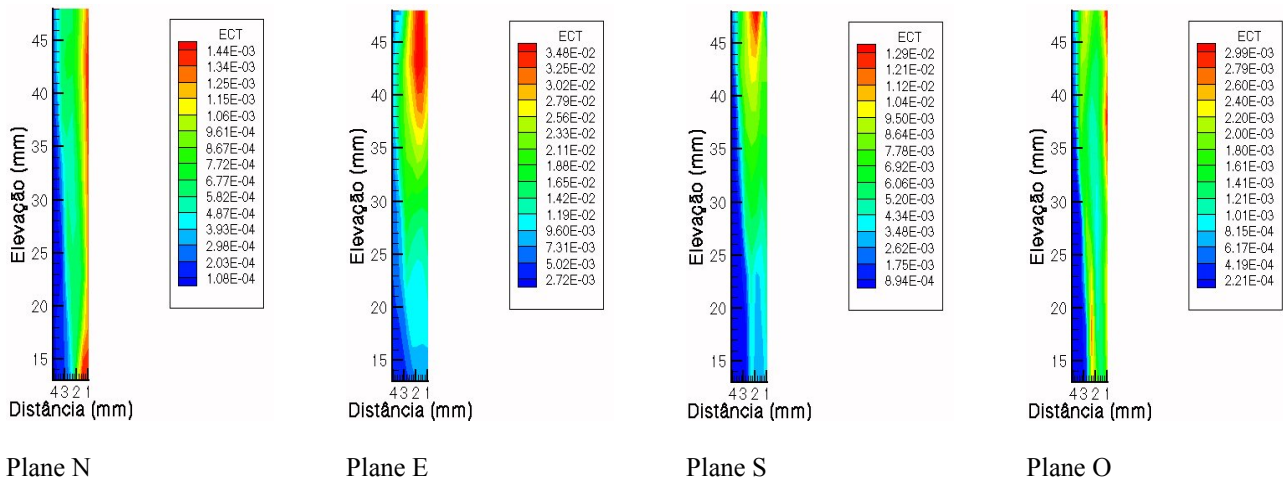


Figure 11 – Turbulent kinetic energy ( $m^2/s^2$ ) in the four planes

The turbulent shear stress distribution in the four planes is shown in figure 12. In the plane N the shear stress decreases radially. In planes S and O the shear stress has a maximum value at the central part of the inlet channel and decreases near the wall and filtering element. In the plane E the stress is maximum at the higher elevation, as the turbulent kinetic energy, due to the presence of the jet. The maximum value observed was 32.4 Pa in plane O.

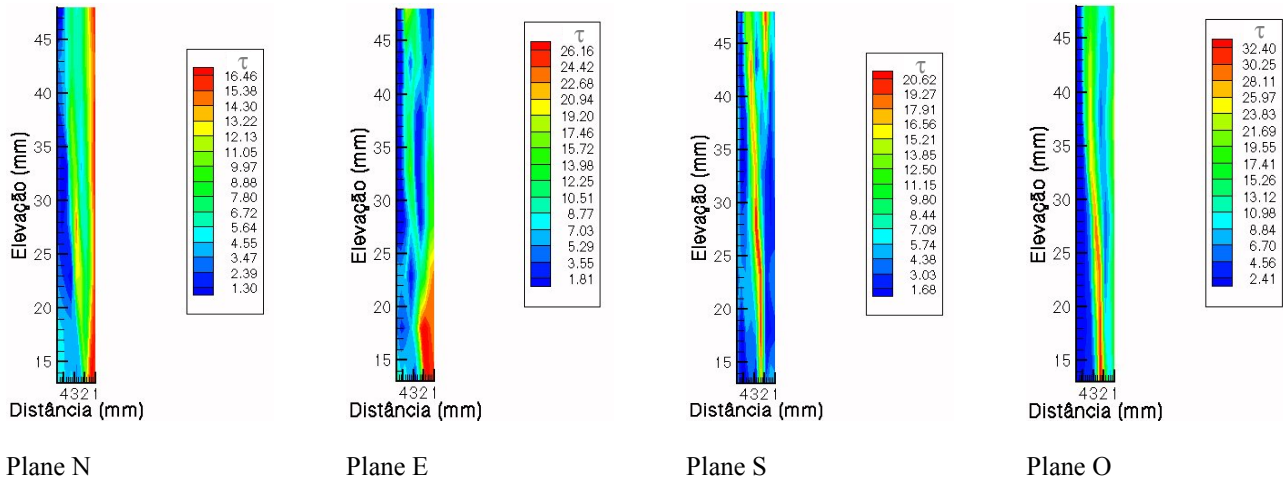


Figure 12 – Turbulent shear stress (Pa) in the four planes

Finally the percentage of released hemoglobin is shown in figure 13. The maximum value was observed near the region where the turbulent shear stress presented a maximum value. The maximum value of released hemoglobin is  $1.43e^{-02}$  and indicates a very low hemolytic potential considering the measured planes.

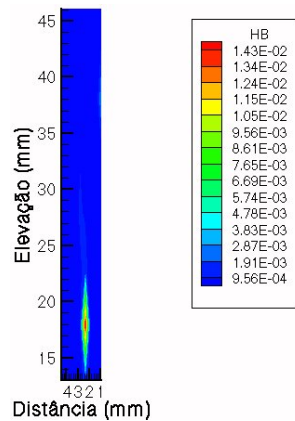


Figure 13 – Percentage of released hemoglobin in plane O

#### 4. Conclusions

This work reports the use of laser Doppler velocimetry to study the flow inside an arterial blood filter. A test bench was developed in order to allow the use of a LDA system and a working fluid with viscosity and density similar those of blood was used. Velocities profiles and their fluctuations were measured at four planes and results show that the flow structure is influenced by the incoming flow in the filter. Velocity fluctuations were used to evaluate turbulent shear stresses which were combined with the exposure time in order to evaluate the percentage of released hemoglobin. Results show also this filter has a low tendency to damage red blood cells, considering the measured planes. The flow was visualized using the dye injection technique and the results are in agreement with the LDA measurements.

#### 5. Acknowledgement

This work was financed by CNPq (Brazilian research council), grants n°200729/95-0 and n°300556/97-7. The contribution of S. Evangelisti to the LDA measurements and V. Ponzio to the construction of the experimental setup is gratefully acknowledged.

#### 6. References

- Baldwin, J.T., Deutsch, S., Petrie, H.L. & Tarbell, J.M., 1993, Determination of principal Reynolds stresses in pulsatile flows after elliptical filtering of discrete velocity measurements. *Journal of Biomechanical Engineering*, v.115, p.396-403.
- Dybbs, A, and Edwards, R.V., 1987, Refractive index matching for difficult situations. *Laser anemometry advances and applications*.
- Higdon, A., Ohlsen, E.H., Stiles, W.B., Weese, J.A. and Riley, W.F., 1985, *Mechanics of Materials*. New York, NY : John Wiley & Sons.
- Paul, R., Schügner, F., Reul, H., Rau, G., (1999), "Recent findings on flow induced blood damage : critical shear stresses and exposure times obtained with a high shear Couette-system", *Artificial Organs*, v.23, n.7, p.680.
- Rand, R.P., 1964, "Mechanical properties of red cell membrane. Part 2, Viscoelastic breakdown of the membrane", *Biophysics*, v.4, p.303-316.
- Sallam, A.M., Hwang, N.H.C., 1984, "Human red blood cell hemolysis in a turbulent shear flow : contribution of Reynolds shear stresses", *Biorheology*, v.21, p.783-797.
- Sutera, S.P., 1977, "Flow induced trauma to blood cells", *Circulation research*, v.41, n.1, p.2-8.
- Sutera, S.P., Mehrjardi, M.H., 1975, "Deformation and fragmentation of human red blood cells in turbulent shear flow", *Biophysical journal*, v.15, p. 1-10.
- Waaben, J., Sørensen, H.R., Andersen, U.L.S., Gefke, K., Lund, J., Aggestrup, S., Husum, B., Laursen, H., Gjedde, A. 1994, "Arterial line filtration protects brain microcirculation during cardiopulmonary bypass in the pig", *The journal of Thoracic and Cardiovascular Surgery*, v.107, n.4, p. 1030-1035.
- Wurzinger, L.J., Opitz, R., Blasberg, P. e Schönbein, S., 1985, Platelet an coagulation parameters following millisecond exposure to laminar shear stress. *Thrombosis and Haemostasis*, v.54, n.2, p.381-386.

#### 7. Copyright Notice

The authors are the only responsible for the printed material included in his paper.